Cryo Cooler Induced Micro-Vibration Disturbances to the Hubble Space Telescope

N. Jedrich[a], D. Zimbelman[b], M. Turczyn[c], J. Sills[d], C. Voorhees[e], B. Clapp[f]

Jackson & Tull 7375 Executive Place Suite 200 Seabrook MD 20706[a], NASA Goddard Space Flight Center Greenbelt MD 20771[b,c], United Space Alliance 1150 Gemini Houston TX 77058-2708[d], Lockheed Martin Commercial Space CPC 100 Campus Drive Newtown PA 18940[e], Lockheed Martin Technical Operations 7474 Greenway Center Drive Suite 200 Greenbelt MD 20770[f]

Abstract

This paper presents an overview of the Hubble Space Telescope (HST) Near Infrared Camera and Multi-Object Spectrometer (NICMOS) Cryo Cooler (NCC) system, a description of the micro-vibration characterization testing performed, and a discussion of the simulated performance. The NCC is a reverse Brayton cycle system that employs micro turbo-machinery to provide cooling to the NICMOS instrument. Extensive testing was conducted to quantify the expected on-orbit disturbances caused by the micro turbo-machinery and provide input to a flexible-body dynamic simulation to demonstrate compliance with the HST 7 milli-arc-second root mean square jitter requirement.

Introduction

NICMOS Instrument

The Near Infrared Camera and Multi-Object Spectrometer (NICMOS) scientific instrument was installed in the aft shroud portion of the Hubble Space Telescope (HST) in 1997. Using three Infrared (IR) cameras, NICMOS provides the only IR imaging (0.8 and 2.5 microns) capability to HST and is located in axial bay 2 as shown in Figure 1.

All three cameras are mounted to a cold optics bench enclosed in a solid nitrogen/aluminum foam dewar that maintains the cameras at 58 ± 2K with a stability of ± 2K. Three thermal shields that surround the dewar provide cooling: the Vapor Cooled Shield (VCS), the Thermo Electric-Cooled Inner Shield, and the Thermo Electric-Cooled Outer Shield as shown in Figure 2. Following HST installation, an unexpected heat load (422 milli-Watts) was identified that reduced the dewar lifetime from a 60 to 22 months. Investigation identified a thermal short between the dewar forward closure cover and the VCS due to thermal expansion of
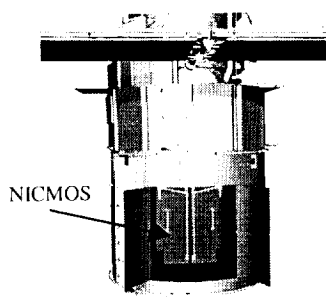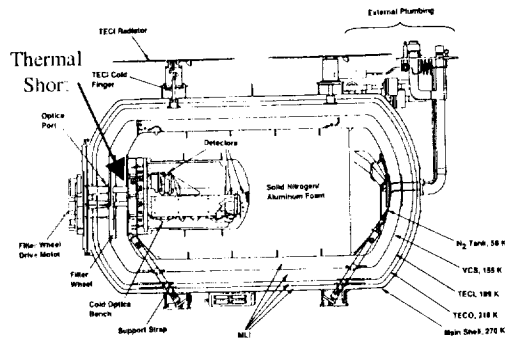
Figure 1 - HST with NICMOS
Installed in Bay 2

Figure 2 - NICMOS Dewar Configuration

the solid nitrogen. In response to the rapid depletion of cryogen caused by the thermal short, an accelerated NICMOS scientific program was implemented to satisfy the primary science objectives.

NICMOS Cryo Cooler

The NICMOS Cryo Cooler (NCC) provides a long-term solution that restores NICMOS scientific operations. The NCC was designed as part of an instrument cooling system that interfaces to existing NICMOS hardware and is scheduled for installation in February 2002. NCC development was driven by two dominant requirements; a 0.77 milli-arc-second (mas) root mean square (rms) jitter allocation out of the HST system level 7 mas rms requirement, and a stable detector temperature of 75 ± 0.5K. The system also had to satisfy all HST mechanical, electrical, and pointing performance requirements. The stringent dynamic stability specification excluded existing cryo cooler technologies and lead to the development of a new mechanical design employing gas bearing turbo-machinery.

The NCC consists of two fluid cooling loops, circulator and cryo cooler, that dump heat from NICMOS to an external radiator as shown in Figures 3 and 4. Figure 5 shows the NCC flight unit adjacent to a NICMOS mockup. The circulating loop uses a centrifugal circulator operating at 1200 revolutions per second (rps) to pump neon, in a continuous steady flow, between the cryo cooler and the NICMOS instrument. The interface from the NCC to the NICMOS coolant loop consists of a pair of titanium bayonets attached to stainless steel flexible lines that connect to an existing NICMOS coolant loop (originally used to freeze the cryogen). Heat is transferred to the cryo cooler loop via the Cold Load Interface, a minimum pressure loss counterflow heat exchanger. The cryo cooler loop is a single stage reverse Brayton cycle design that utilizes turbo-machinery in both the compression and expansion processes. Refrigeration is provided by expansion of the gas across the turbine rotor of the turboalternator. The resulting shaft work is converted to electric power by the alternator, conveyed to a resistive load, and ultimately dissipated as heat at the Heat Rejection Interface (HRI). At the warm end of the loop, a centrifugal compressor operating at up to 7500 rps provides compression.

Compression heat is rejected via the HRI to a third, external cooling loop, and transferred to space. The recuperator provides efficient heat transfer between the high and low-pressure streams of gas[1]

The gas bearing design and small rotor mass of the micro turbo-machinery results in an extremely efficient and relatively vibration free system. Two factors separate the compressor dynamic behavior from either the turbolternator or circulator, the increased mass of the shaft combined with higher operator speeds and a "surging" phenomenon. Surging occurs during warm startup conditions when flow in the system is reduced below nominal operating conditions resulting in compressor pressure oscillations. The magnitude and frequency of these oscillations are dependent on system flow impedance characteristics and the temperature of the fluid at the cold end.

Figure 3 - NICMOS Cryo Cooler

Figure 4 - NICMOS Cooling System

Disturbance Requirements and Initial Test Results

The requirement was derived that the cooling system (including the external radiator) should contribute no more than 1 mas rms jitter above the current HST pointing performance level of 3 mas rms. Of the 1 mas rms jitter allocation, 0.77 mas rms jitter is allotted for NCC induced disturbances as previously stated.

Initial testing of the NCC included on-orbit disturbance measurements recorded during the Hubble Orbital Systems Test (HOST) mission. Unfortunately, NCC disturbance measurements from HOST[5] were influenced by orbiter payload operations and low-frequency astronaut activity onboard the space shuttle. The flight data predicted NCC induced jitter of 27 mas rms and 4.5 mas rms during surging and steady state operation respectively. The only significant jitter result obtained was qualitative: NCC induced disturbances at steady state are always lower than during surging. The HOST mission data set contained large random and systematic errors resulting in the need for a state-of-the-art, ground-based Vibration Emittance Test (VET).

Vibration Emittance Test

The VET characterizes very low-frequency disturbances by measuring NCC induced vibrations at ambient temperatures in an ultra low-noise facility. The surging test data set provides an enveloping case for induced disturbances during all phases of operation.

Background Noise Measurements and Support Equipment

The Reverberant Acoustic Test Facility was selected to perform the NCC VET based on extremely low background noise measurements. Two accelerometers, the PCB 393 seismic and the QA-2000 servo, were used to obtain background noise levels. Low-frequency results (0 to 5 Hz) showed a maximum measured background noise of 200 nano-g.

The Mechanical Ground Support Equipment (MGSE) was designed to accommodate three CSA Engineering 40350-0-V Zero-G Suspension Devices (ZGSDs) and was secured against the ceiling using a crane and stabilized to within 1 degree of parallel by four support posts. The NCC was attached to each ZGSD carriage by braided Kevlar (9.14 m length) as shown in Figure 6. The ZGSD was only used for structural support as their operation introduced additional low-frequency noise created by fluctuations in the facility air supply system.
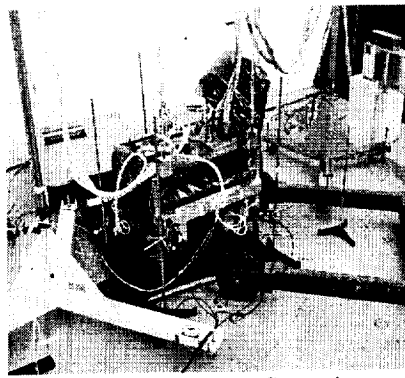

Figure 5 - NCC Flight Unit

Figure 6 - VET Configuration

Instrumentation and Data Acquisition

Measurement instrumentation employed in the test is listed in Table 1. Compensation circuitry for thermal and 1-g effects acting on the servo accelerometers was developed and implemented for all aspects of the test[2]. The data acquisition system used to record accelerometer, force gage, and displacement data, was a 64-channel Pacific Instruments 600 DAS unit. Each channel of the system utilized a 4-pole Butterworth anti-aliasing filter compatible with plug-in filter

frequency cutoffs. Previous testing with this system determined that 100% alias free data is not practical due to very large block size requirements with the filter. It was determined that a frequency ratio of 8 between the sampling and filter cutoff frequency would produce only a 1.5% error in the Power Spectrum Density. Given the duration for each test sequence (~15 minutes), the sample rate for all acquired signals was set to 160 Hz to minimize any anti-aliasing of data and the block rate was chosen by multiplying the highest filter cutoff frequency for a given channel by the frequency ratio.

Type	Location	Function
12 Allied Signal QA-2000 Accelerometers	NCC (3 clusters of 4)	Measure rigid body dynamics
6 Kamen KD2300-10CU Eddy Current Probes	Near NCC accelerometers	Measure rigid body dynamics
6 Kistler Tri-Axial Piezobeam 8692B5M1 Accelerometers	MGSE frame	Measure facility background noise
3 PCB Model 201B03 Force Gauges	NCC lift points	Measure mass distribution

Table 1 – Instrumentation Specification

Disturbance Measurements

The test setup resulted in lateral suspension frequencies of 0.21 Hz and 0.25 Hz and a torsional suspension frequency of 0.45 Hz. NCC accelerations measured above these frequencies by the servo accelerometers were proportional to the disturbance forces, where the proportionality constant was the NCC VET system mass. Below the suspension frequencies, acceleration is not proportional to the disturbance force and no signatures were measured that exceeded the noise floor. Figure 7 shows the spectral content of the NCC induced surging disturbances measured during the VET with the background noise superimposed on the same graph. Measured acceleration background noise was 7 micro-g rms along the long-axis of the NCC with the NCC off, while the measured acceleration was 19 micro-g rms with the NCC surging at a compressor speed of 5800 rps. The two other translational acceleration components were of similar magnitude, while the rotational accelerations were insignificant by comparison. As shown in Figure 7, NCC disturbances during surging are characterized by significant spectral content at 3.5 Hz and higher integer multiples of this fundamental surging frequency.

HST Pointing Performance

Attitude Control System and Disturbance Rejection Characteristics

The HST attitude control system[3] uses a classical proportional-integral-derivative law to actuate reaction wheels based on Rate Sensor Unit (RSU) measurements. Fine guidance sensors are used for inertial attitude measurement to correct for RSU

drift via an attitude observer. Currently, the control system achieves 2-3 mas rms pointing stability over 60 second intervals in the presence of various on-orbit disturbances acting on the vehicle. Following launch, the control system software was modified[4] to provide additional attenuation at the solar array structural modes.

HST will undergo significant configuration changes, following Servicing Mission 3B (SM3B), by replacing the blanket type arrays with a pair of rigid arrays, and the inclusion of the NCC. Similarly, the HST attitude control law gains will be configured to the original values set at initial deployment. A disturbance rejection transfer function in the post-SM3B configuration is shown in Figure 8 that represents the HST rotational response about the transverse vehicle axis due to NCC long-axis force input. This is one of 12 transfer functions characterizing the effects of NCC disturbances upon HST pointing errors. HST pointing performance is particularly sensitive to low-frequency disturbances in the 0.02 Hz to 0.5 Hz frequency range as evident in Figure 8. Thus measuring low-frequency NCC induced disturbances was a primary goal of the VET. The resonant peaks shown in Figure 8 illustrate the fidelity of the pointing control system simulation models, as the influence of all HST flexible appendage modes below 50 Hz is shown.

Pointing Performance Assessment

The predicted pointing performance for the HST post-SM3B configuration was computed using two independent methods. The first applied linear frequency domain methods to compute HST boresight jitter and uncertainties due to the NCC and other disturbance sources acting independently. The second technique used a high-fidelity, non-linear, time-domain simulation to estimate overall HST performance during fine pointing in the presence of all disturbance sources acting concurrently.
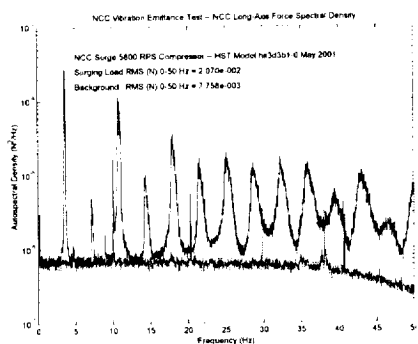

Figure 7 - VET Disturbance Force Autospectrum in the Direction of NCC Long-Axis
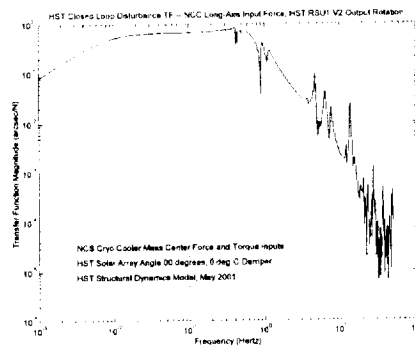

Figure 8 - Post-SM3B HST Disturbance Rejection Transfer Function

The linear frequency domain analysis for NCC induced surging disturbances predicts a HST boresight attitude error of 3.64 mas rms. NCC induced surging disturbances incorporated a 20% uncertainty factor to account for random and systematic errors associated with the VET. High-fidelity simulation results estimate 3.05 mas rms HST boresight attitude error due to all disturbances with the NCC surging operation as the dominant source. Although NCC steady-state disturbances were not characterized, estimated HST boresight attitude error during this operation is 2.26 mas rms.

Conclusion

The NCC, as designed, will restore NICMOS science while satisfying all HST requirements. The VET successfully demonstrated the capability to measure low-frequency NCC induced micro-dynamic disturbances in an ultra low-noise environment. Detailed analysis of the VET data predicts that NCC induced disturbance errors will meet the stringent HST pointing performance.

References

1. Nellis, G., Dolan, F., McCormick, J., Swift, W., Sixsmith, H., Gibbon, J., and Castles, S., Reverse Brayton Cryo Cooler for NICMOS, *Cryocoolers 10*, New York, Kluwer Academic Publishers, 1999.
2. Voorhees C.R., Sills J.W. and Clapp B., A System for Microgravity Measurements on the HST NCC Vib Emittance Test, *71st Shock and Vibration Symposium*, SAVIAC, November 2000.
3. Dougherty, H., Tompetrini, K., Levinthal, J., and Nurre, G., Space Telescope Pointing Control System, *Journal of Guidance, Control, and Dynamics*, vol. 5, no. 4, pp.403-409, 1982.
4. Sharkey J. P., Nurre G. S., Beals G. A. and Nelson J. D., A Chronology of the On-orbit Pointing Control System Changes on the Hubble Space Telescope and Associated Pointing Improvements, *AIAA Paper 92-4618*, August 1992.
5. Story D., Cofie E., Clapp B. and Cepollina F., Of the NASA Hubble Space Telescope (HST) Near Infrared Camera Multi-Object Spectrometer (NICMOS) Cryogenic Cooler (NCC) in a Microgravity Environment, *52nd International Astronautical Congress*, Toulouse, France, October 2001.